Electronic Structure and Dynamics of Quantum-Well States in Thin Yb Metal Films

D. Wegner, A. Bauer, and G. Kaindl

Institut für Experimentalphysik, Freie Universität Berlin, Arnimallee 14, 14195 Berlin-Dahlem, Germany

(Received 8 November 2004; published 1 April 2005)

Quantum-well states above the Fermi energy in thin Yb(111) metal films deposited on a W(110) single crystal were studied by low-temperature scanning tunneling spectroscopy. These states are laterally highly localized and give rise to sharp peaks in the tunneling spectra. A quantitative analysis of the spectra yields the bulk-band dispersion in the Γ-L direction as well as quasiparticle lifetimes. The quadratic energy dependence of the lifetimes is in quantitative agreement with Fermi-liquid theory.

DOI: 10.1103/PhysRevLett.94.126804 PACS numbers: 73.21.Fg, 68.37.Ef, 71.20.Eh, 73.50.Gr

Quantum-well states in thin metal films have been studied for noble metals, alkali metals, and a few other metals, mostly by laterally averaging experimental techniques such as photoemission or inverse photoemission that probe the occupied and unoccupied electronic structure, respectively [1,2]. Since these techniques are laterally averaging, they require highly homogeneous films with unique thickness over the sampled area of ≈ 0.1 mm. A different approach is opened by scanning tunneling spectroscopy (STS) and microscopy (STM), with lateral resolution on the atomic scale, and a few studies have made use of these techniques [3–8].

Spectroscopic studies yield both the energy and the lifetime width of quantum-well states and are particularly suited for the study of quasiparticle lifetimes in the respective materials [9–11]. For nonmagnetic materials, in the absence of defects, the quasiparticle lifetimes are mainly determined by electron-electron (e-e) and electron-phonon (e-ph) scattering. These processes can be distinguished by different temperature and energy dependences. For energies relative to the Fermi energy, E_F, that are larger than the Debye energy, e-ph scattering rates are nearly energy independent [12]. On the other hand, e-e scattering is expected to show a quadratic energy dependence according to Fermi-liquid theory [13], which had indeed been observed for quantum-well states in Ag films [9,10]. While for noble metals, a good understanding of quasiparticle lifetimes has been achieved by now [14,15], the situation is quite different for transition metals with their more complex electronic structures.

In the present Letter we report on an extensive STS study of quantum-well states in thin Yb(111) films grown on W(110) in the thickness region from 9 to 23 monolayers (ML). The well-resolved STS spectra can be described quantitatively by a superposition of thermally broadened Lorentzian lines with lifetime widths Γ that depend quadratically on the energy above E_F, in accordance with Fermi-liquid theory, plus a constant offset due to e-ph scattering. From the energies of the quantum-well peaks as a function of film thickness, the bulk-band dispersion along Γ-L is derived in a 1.5-eV energy region above E_F. The results provide, for the first time, detailed insight into hot-electron dynamics in lanthanide metals.

Yb is a divalent lanthanide metal with filled $4f$ shell crystallizing in the fcc structure. According to band-structure calculations, the bulk band disperses downwards between the Γ and L points, i.e., perpendicular to the (111) plane, with a total width of ≈ 2.5 eV. By angle-resolved photoemission, the band minimum was determined at 80 meV below E_F, in agreement with the present STS results, while band-structure calculations put it 0.1 eV above E_F [16,17]. This band has a very small dispersion parallel to the (111) plane, which makes it an ideal candidate for STS studies, since STS does not readily provide k resolution. A prerequisite for the existence of quantum-well states in a thin film is a small or vanishing hybridization of the electronic states of film and substrate. Although there is no band gap in W(110) at $\overline{\Gamma}$ above E_F, the hybridization of states at $\overline{\Gamma}$ is small due to different symmetries.

The experiments were performed in an ultrahigh vacuum chamber equipped with a low-temperature STM operated at 10 K [18]. The samples were prepared *in situ* by electron-beam evaporation of Yb and deposition on a clean W(110) single crystal kept at room temperature. A quartz microbalance was used to monitor the average thickness of the deposited film. STM images were taken in constant-current mode, and the STS spectra were recorded with fixed tip position, i.e., switched off feedback control. The conductivity, dI/dU, with I being the tunneling current and U the sample bias voltage, was recorded as a function of U by modulating U and recording the induced modulation of I via the lock-in technique. In good approximation, dI/dU is proportional to the density of states at the sample surface. A modulation amplitude of 1 mV (rms) at a frequency of ≈ 360 Hz was used, with the time constant of the lock-in amplifier set to 100 ms, at a sweep rate of ≈ 6 mV/s. The spectra were taken in both directions, from lower to higher and from higher to lower sample bias, in order to correct for binding energy shifts due to the finite time constant. Since both the STM tip and the sample were cooled to 10 K, the energy resolution was ≈ 3 meV, corresponding to $3.5k_BT$.

In Fig. 1, STM images of Yb/W(110) films are displayed for three average film thicknesses. The films were found to be rather rough, with local thickness variations up to $\pm 30\%$. Locally, however, the films were atomically flat, with terraces several tens of nanometers wide. Two kinds of dislocation lines are visible on the terraces: (i) Small steps running diagonally through the images [best seen in Fig. 1(d)] that result from buried monatomic steps on the W(110) surface. The observed step height of ≈ 0.9 Å corresponds to the difference in the layer spacings of Yb(111) (3.17 Å) and W(110) (2.23 Å). In Fig. 1(d), e.g., the local film thickness decreases from the upper left corner to the lower right corner by 3 ML. (ii) More irregularly shaped lines that appear as trenches and come in pairs. They represent dislocations that result from the lattice mismatch between Yb(111) and W(110). The density of these dislocations decreases with increasing film thickness [compare Figs. 1(d)–1(f)]. The area enclosed by a pair of lines has most likely hcp structure, i.e., a different stacking sequence than the fcc structure of the surrounding film. Similar dislocations had been observed before for other thin-film systems [19]. A more detailed description of these dislocations and of their influence on quantum-well states will be published elsewhere [20].

Considering the morphology of the Yb/W(110) films, it appears impossible to observe quantum-well states in this case with a laterally averaging technique. With STS, however, we were able to measure quantum-well states for various film thicknesses with just one sample. We could even record spectra for different local thicknesses on a single Yb(111) terrace with buried W(110) steps underneath. Lateral confinement effects on the electronic structure of the quantum wells were observed only for distances smaller than 40 Å from steps or dislocation lines [20], a fact that indicates a high degree of lateral localization of the quantum-well states. Figure 2 displays representative STS spectra for local film thicknesses between 9 and 23 ML. There is a systematic uncertainty in the thickness of ± 1 ML that is not relevant, however, for the following analysis, since only differences in thickness enter the equations.

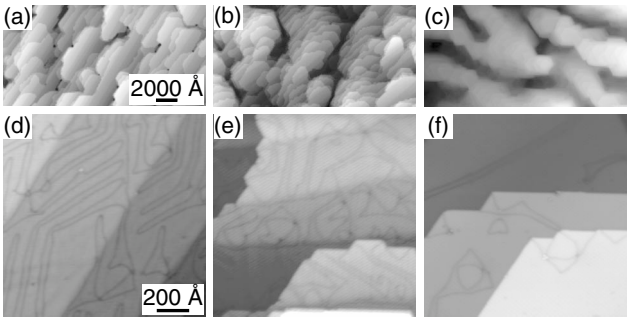

FIG. 1. STM images of Yb/W(110) films with average thicknesses of (a),(d) 12 ML, (b),(e) 20 ML, and (c),(f) 130 ML.

Each spectrum consists of a series of relatively sharp peaks that reflect the formation of quantum-well states. With increasing film thickness, the distances between the peaks decrease and more peaks appear. For rather thick films, a continuous band forms, and a steplike feature is observed (see the inset in Fig. 2) that represents the bottom of the band at $E - E_F = eU = -80$ meV, in agreement with previous photoemission studies [16]. The spectra measured for negative sample bias are often superimposed by tip-induced features that could not be eliminated in a reproducible way, even after tip cleaning by field emission. Therefore only the peaks observed for positive sample bias, $U > 50$ mV, are analyzed here.

A superposition of Lorentzian lines was least-squares fitted to each tunneling spectrum [see Fig. 3(a)]. Thermal broadening was accounted for by convolution with the derivative of the Fermi-distribution function at 10 K [18]. Peak positions, i.e., energies of quantum-well states, are plotted in Fig. 3(b). The dependence of the energies E of

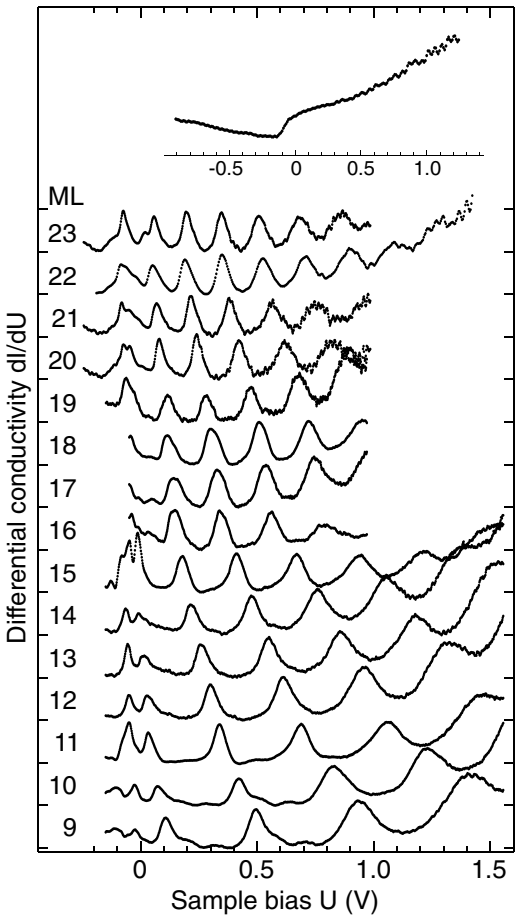

FIG. 2. Tunneling spectra of Yb/W(110) films with various local thicknesses. The spectra were recorded on 2 different samples with an average film thickness of 12 ML (varying locally between 9 and 15 ML) and 20 ML (16–23 ML), respectively. Inset: Tunneling spectrum of a 130-ML-thick Yb/W(110) film.

these quantum-well states on film thickness allows one to derive the Γ-L band dispersion. To this end, the Bohr-Sommerfeld quantization rule for quantum-well states is used [21]:

$$2k_\perp(E)d + \delta(E) = 2\pi n, \quad (1)$$

with $k_\perp$ representing the k value perpendicular to the film plane, d the film thickness, δ the phase shift due to reflection at the two interfaces, and n the number of the quantum-well state. For two states n and n' with the same energy E for film thicknesses d and d', one obtains

$$k_\perp = \pi(n - n')/(d - d'). \quad (2)$$

These equations assume the band minimum to occur at Γ, while band-structure calculations show that it occurs at the L point [17]. Therefore, $k_\perp$ has to be replaced by $k_L - k_\perp$ [22]. For the calculation of $k_\perp(E)$ with Eq. (2), the experimental data points $E_n(d)$ were interpolated as shown by the solid curves in Fig. 3(b). The analysis then results in the band dispersion given in Fig. 3(c) by solid points with error bars. The results of the band-structure calculations of Ref. [17] reproduce the experimental data only roughly, with increasing deviations when the L point is approached [solid line in Fig. 3(c)]; in addition, these calculations find the band minimum more than 100 meV above E_F, while the experiment clearly puts it at 80 meV below E_F.

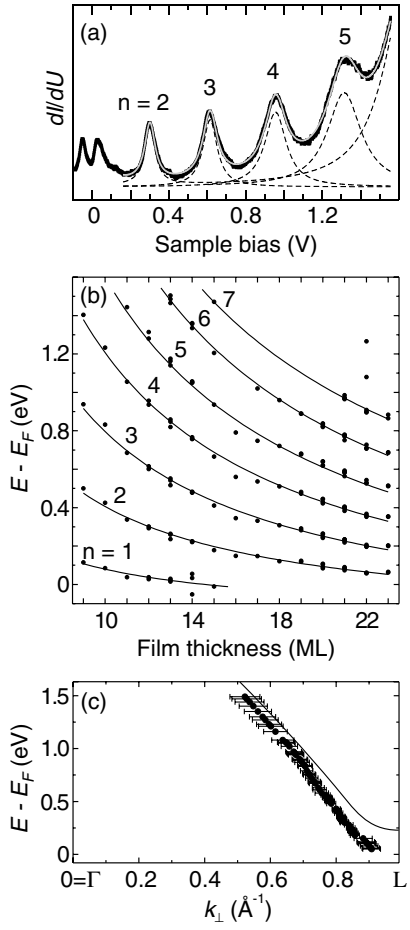

FIG. 3. (a) Least-squares fit (solid line) of a superposition of thermally broadened Lorentzian lines (dashed line) to the 12-ML Yb/W(110) tunneling spectrum. (b) Energies of quantum-well states in Yb/W(110) for various film thicknesses. To get binding energies for noninteger multiples of Yb monolayers, the experimental data were interpolated (solid lines). (c) Energy dispersion of the Yb bulk band along Γ-L within reciprocal space as determined from the thickness dependence of the quantum-well binding energies. The solid line is the result of a band-structure calculation [17].

In the following, we discuss the linewidths of the quantum-well states displayed in Fig. 4. They allow us to derive quasiparticle lifetimes of hot electrons in Yb metal over a relatively large energy region. As shown in Fig. 3(a), the peaks in the tunneling spectra are well described by Lorentzian lines. If there are no other line-broadening effects in the Yb film but quasiparticle scattering, the lifetimes of the quantum-well states, τ, are obtained by $\tau = \hbar/\Gamma$, where the Γ represent the width (FWHM) of the Lorentzian lines derived from the fit procedure [see Fig. 3(a)].

Other broadening mechanisms, however, have to be taken into account as well. They include lateral dispersion of the quantum-well states and electron transmission to the W(110) substrate. The first mechanism can be neglected since a sizable dispersion of the states would result in asymmetric line shapes [18] that are not observed; contributions to the linewidths from lateral dispersion are estimated to be ≤ 10 meV. This is supported by band-structure calculations that show a rather flat dispersion parallel to the (111) surface [16]. Transmission to the W(110) substrate is also rather small since the linewidths of quantum-well states at given energies were found to be independent of film thickness within the error bars. We further assume that contributions of substrate transmission to the linewidth decrease with increasing film thickness when the interface has less and less influence on the electronic structure of the film, expectedly with a $1/d$

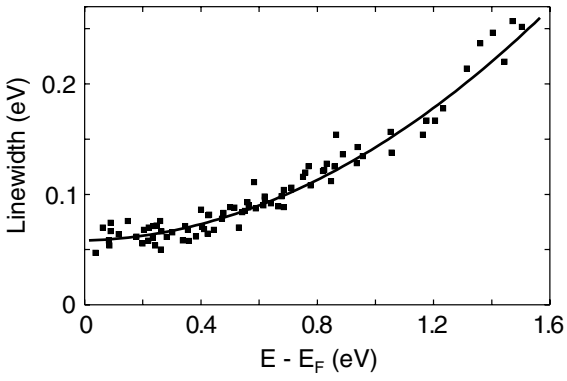

FIG. 4. Linewidths of quantum-well states in Yb/W(110) as a function of energy above E_F. The solid line represents the result of a fit of a 2nd-order polynomial to the data.

dependence [10]. The linewidth data, with error bars of ± 10 meV, are then consistent with a transmission of up to 20% at the Yb/W(110) interface. To arrive at this conclusion, we followed Ref. [10], where it was shown that the linewidth Γ is given by $\Gamma = f\hbar/\tau$, with $f = 1$ for zero transmission and $f = 1.7$ for 20% transmission.

The data in Fig. 4 are well described by a quadratic function (solid line in Fig. 4):

$$\Gamma = \Gamma_0 + \Gamma_2(E - E_F)^2, \quad (3)$$

with $\Gamma_0 = (58 \pm 3)$ meV and $\Gamma_2 = (0.079 \pm 0.008)$ eV^{-1}. Γ_0 is attributed to lifetime width due to e-ph scattering, which is expected to depend only slightly on energy [12]. Assuming $\Gamma_0/f = 2\pi\lambda\hbar\omega_D/3$ [12] and a value of $\hbar\omega_D = 10$ meV for the Debye frequency of Yb metal [23], we obtain for the electron-phonon mass-enhancement factor λ values between $\lambda = 1.6$ for 20% transmission and $\lambda = 2.8$ for zero transmission. These values indicate strong electron-phonon interaction in Yb metal. Similar values for λ, although not quite as large, have previously been obtained for other trivalent lanthanide metals such as Gd and Lu [24,25]. We note that more detailed information on e-ph scattering, in particular, a possible energy dependence of λ, can be obtained from temperature-dependent measurements [11,25,26].

The quadratic term in Eq. (3) is supposed to result from e-e scattering, with $\Gamma_2/f = 2\beta = 0.0025 r_s^{5/2}$ eV^{-1} [13]; here, r_s is the electron-density parameter. For Yb, with $r_s = 3.21$, one obtains $2\beta = 0.046$ eV^{-1}, a value that agrees very well with the experimental value for 20% transmission: $2\beta_{\mathrm{exp}}(f = 1.7) = (0.046 \pm 0.005)$ eV^{-1}. The observation of a quadratic energy dependence as well as the quantitative agreement of the value of Γ_2 with the prediction for the e-e scattering strength is rather astonishing since it has not been clear up to now whether the simple Fermi-liquid model by Quinn and Ferrell [13] is applicable to lanthanide metals. Deviations from a quadratic energy dependence have been reported for several $3d$-transition metals [27], where the conduction electrons, however, are much stronger correlated than in the heavy lanthanide metals. The present results stimulate further studies on other lanthanides and highly correlated materials.

This work was supported by the Deutsche Forschungsgemeinschaft, Project No. Sfb-290/TPA6. A. B. acknowledges support within the Heisenberg program of the Deutsche Forschungsgemeinschaft.

[1] T.-C. Chiang, Surf. Sci. Rep. **39**, 181 (2000).
[2] M. Milun, P. Pervan, and D. P. Woodruff, Rep. Prog. Phys. **65**, 99 (2002).
[3] M. Schmid *et al.*, Phys. Rev. Lett. **76**, 2298 (1996).
[4] I. B. Altfeder, K. A. Matveev, and D. M. Chen, Phys. Rev. Lett. **78**, 2815 (1997).
[5] R. Otero, A. L. V. de Parga, and R. Miranda, Surf. Sci. **447**, 143 (2000).
[6] W. B. Su *et al.*, Phys. Rev. Lett. **86**, 5116 (2001).
[7] I. B. Altfeder, V. Narayanamurti, and D. M. Chen, Phys. Rev. Lett. **88**, 206801 (2002).
[8] H. Yu *et al.*, Appl. Phys. Lett. **81**, 2005 (2002).
[9] J. J. Paggel, T. Miller, and T.-C. Chiang, Phys. Rev. Lett. **81**, 5632 (1998).
[10] J. J. Paggel, T. Miller, and T.-C. Chiang, Science **283**, 1709 (1999).
[11] D.-A. Luh *et al.*, Phys. Rev. Lett. **88**, 256802 (2002).
[12] G. Grimvall, *The Electron-Phonon Interaction in Metals* (North-Holland, New York, 1981).
[13] J. J. Quinn and R. A. Ferrell, Phys. Rev. **112**, 812 (1958).
[14] L. Vitali *et al.*, Surf. Sci. **523**, L47 (2003).
[15] P. M. Echenique *et al.*, Surf. Sci. Rep. **52**, 219 (2004).
[16] M. Bodenbach *et al.*, Phys. Rev. B **50**, 14 446 (1994).
[17] G. Johansen and A. R. Mackintosh, Solid State Commun. **8**, 121 (1970).
[18] A. Bauer *et al.*, Phys. Rev. B **65**, 75 421 (2002).
[19] C. Günther *et al.*, Phys. Rev. Lett. **74**, 754 (1995).
[20] D. Wegner, A. Bauer, and G. Kaindl (unpublished).
[21] M. A. Mueller, T. Miller, and T.-C. Chiang, Phys. Rev. B **41**, 5214 (1990).
[22] J. E. Ortega and F. J. Himpsel, Phys. Rev. Lett. **69**, 844 (1992).
[23] T. E. Scott, in *Handbook on Physics and Chemistry of Rare Earths*, edited by K. A. Gschneidner, Jr. and L. Eyring (North-Holland, Amsterdam, 1978), Vol. 1.
[24] H. L. Skriver and I. Mertig, Phys. Rev. B **41**, 6553 (1990).
[25] A. Rehbein *et al.*, Phys. Rev. B **67**, 33403 (2003).
[26] J. E. Gayone *et al.*, Phys. Rev. Lett. **91**, 127601 (2003).
[27] A. Goldmann, R. Matzdorf, and F. Theilmann, Surf. Sci. **414**, L932 (1998).